Chemical Science

EDGE ARTICLE

View Article Online
View Journal | View Issue

Cite this: *Chem. Sci.*, 2016, **7**, 774

A wavelength-resolved ratiometric photoelectrochemical technique: design and sensing applications†

Qing Hao,[a] Xiaonan Shan,[b] Jianping Lei,*[a] Yang Zang,[a] Qianhui Yang[a] and Huangxian Ju[a]

In this work, a wavelength-resolved ratiometric photoelectrochemical (WR-PEC) technique was investigated and employed to construct a new type of PEC sensor with good sensitivity and anti-interference ability. The WR-PEC hybrid photoelectrodes were stepwise assembled using semiconductor quantum dots (QDs) and photoactive dyes. Under continuous irradiation, the photocurrent–wavelength (I–λ) curves reveal the dependence of the photocurrent on the wavelength. By monitoring the ratios of the two different PEC peak values, a wavelength-resolved ratiometric strategy was realized. Using CdS QDs and methylene blue (MB) as photoactive models, a dual-anodic WR-PEC sensor was established for sensitive detection of Cu^{2+}. This ratiometric strategy was identified to be based on the quenching effect of Cu^{2+} towards CdS QDs and enhancement of the MB photocurrent through catalytic oxidation of leuco-MB. Under continuous illumination from 400 nm to 800 nm at a 0.1 V bias potential, a WR-PEC sensor for Cu^{2+} was developed with a wide linear range and a detection limit of 0.37 nM. This WR-PEC had a greatly improved anti-interference ability in a complex environment, and showed acceptable stability. Moreover, using the CdS/magnesium phthalocyanine (MgPc) and CdTe/MgPc as photoelectrodes, anodic–cathodic and dual-cathodic WR-PEC sensors were established, respectively. The WR-PEC technique could serve as a novel concept for designing ratiometric or multi-channel PEC sensors.

Received 4th September 2015
Accepted 15th October 2015

DOI: 10.1039/c5sc03336e

www.rsc.org/chemicalscience

Introduction

Trace analysis in complex samples requires rapid and accurate modern analytical techniques with a low background and a good anti-interference ability. Therefore, ratiometric techniques have extensively been investigated and applied to electrochemistry,[1–3] photoluminescence (PL),[4–8] and electrochemiluminescence protocols.[9–11] These ratiometric techniques have then significantly improved the analytical efficiency of those traditional analytical techniques. For example, based on a potential-resolved approach, a one-step electrochemical detection of protein was realized using a ratiometric electrochemical proximity assay hybridized from a methylene blue (MB)-labeled antibody-DNA probe and ferrocene-labeled DNA capture probe.[2] Meanwhile, a wavelength-resolved ratiometric fluorescent probe consisting of BODIPY–rhodamine with two separate fluorescence signals, was designed for imaging of Hg^{2+} ions in living cells.[6] Inspired by the similarity between photoelectrochemistry (PEC) and PL, a ratiometric PEC method should improve the sensitivity and anti-interference ability of sensors. Therefore, a wavelength-resolved ratiometric photoelectrochemical (WR-PEC) technique was first designed and then exploited as an ingenious sensor for selective detection of Cu^{2+} in this paper.

PEC, as a novel detection technique in which photocurrent change could be brought about during the recognition process of the target analyte, has been successfully applied to establish a series of biosensors owing to its unique advantages such as good biocompatibility, low background, and high analytical efficiency.[12] To date, conventional PEC biosensors have been based on a single wavelength of light or a white light source using one PEC species.[13–17] Most PEC sensors only provide one output signal, which inevitably limits the sensitivity, anti-interference ability and the detection performance for complex samples. To address these issues, it is desirable to fabricate a ratiometric PEC sensor with two absorption-separated photoactive species. In general, photoactive species including semiconductors such as TiO_2,[18] bismuth oxyiodide,[19] and quantum dots (QDs),[20–23] and photoactive dyes such as Ru complexes,[24] porphyrin,[25,26] phthalocyanine[27,28] and toluidine

[a]*State Key Laboratory of Analytical Chemistry for Life Science, School of Chemistry and Chemical Engineering, Nanjing University, Nanjing 210093, P. R. China. E-mail: jpl@nju.edu.cn; Fax: +86 25 83593593; Tel: +86 25 83593593*

[b]*Center for Bioelectronics and Biosensors, Biodesign Institute, Arizona State University, Tempe, Arizona 85287, USA*

† Electronic supplementary information (ESI) available: Supplementary figures. See DOI: 10.1039/c5sc03336e

blue,[29] have played critical roles in PEC platforms. In particular, QDs have been widely applied in the construction of PEC biosensors due to their distinctive optical and electrochemical properties.[30–32] Considering the separation of the absorption spectra of photoactive dyes and semiconductors, it is feasible to simultaneously output two PEC signals with both QDs and photoactive dyes for development of a WR-PEC sensor.

Herein, using CdS QDs (anodic material) and MB (anodic material) as photoelectrode models, a WR-PEC sensor with better anti-interference ability was constructed by stepwise assembly of CdS QDs and MB on an indium tin oxide (ITO) electrode (Fig. 1). The dual-anodic photoelectrode (DA-PEC) displayed a dependence of photocurrent on wavelength under a continuous spectrum irradiation (Fig. 1A). On the basis of the quenching effect of Cu^{2+} towards CdS QDs and the enhancement of the MB photocurrent through catalytic oxidation of leuco-MB, a wavelength-resolved ratiometric approach was realized. Thus, a Cu^{2+} ratiometric PEC sensor was successfully developed *via* Cu^{2+} induced increased loading of MB (Fig. 1B). More importantly, by using the different types of PEC materials, the CdS QDs/magnesium phthalocyanine (MgPc) photoelectrode and the CdTe QDs/MgPc photoelectrode were expanded as anodic–cathodic and dual-cathodic WR-PEC sensors, respectively. The WR-PEC technique provides a novel concept for the design of ratiometric PEC sensors and demonstrates promising applications in complex samples.

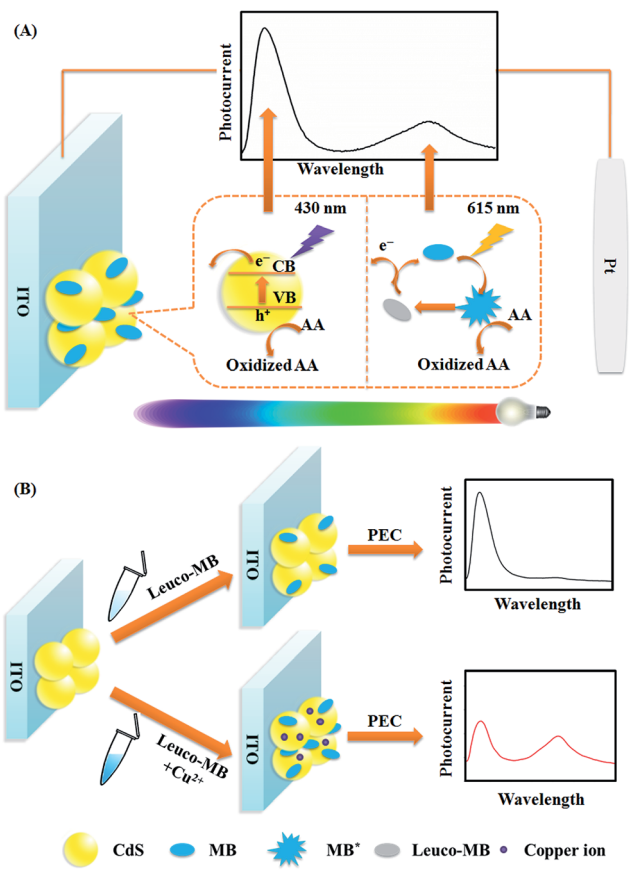

Fig. 1 Schematic illustration of (A) the WR-PEC photocurrent generation process of CdS and MB in a visible light range, and (B) the sensing principle for Cu^{2+}.

Results and discussion

PEC behavior of ratiometric photoelectrode

To remove light below 400 nm, a transmissive filter (UVCUT 400) was placed in the optical system of the PEC platform. The CdS/MB DA-PEC photoelectrode exhibited a photocurrent–wavelength (I–λ) curve in the presence of ascorbic acid (AA) with two separate photocurrent peaks (Fig. 2, curve a). Obviously, these two peaks could easily be related to the I–λ curves of CdS (curve b) and MB (curve c), respectively. The photocurrent around 430 nm was generated through the photo-induced charge separation process of CdS QDs, that is, the electrons in the valence band (VB) were transferred to the conduction band (CB) through absorbing light with energy larger than the band gap, leaving holes in the VB. A part of the photoactive electrons in the CB descended to the ITO electrode, while holes in the VB were scavenged by electron donor AA to realize photogenic charge carrier separation and thus generate photocurrent (Fig. 1A). On the other hand, the photocurrent peak at around 615 nm was generated due to electron transfer of leuco-MB to the surface of the ITO electrode under a 0.1 V bias potential (Fig. 1A), in which excited state MB (MB*) was produced by light irradiation in the absorption band of MB, and was then reduced to leuco-MB by the coreactant AA in the electrolyte.[29,33] The separation of the two photocurrents provides the possibility of establishing a wavelength-resolved ratiometric PEC approach.

Characterization of CdS/MB photoelectrode

Transmission electron micrographs (TEM) were used to characterize the topography and size of the CdS QDs. A typical TEM of CdS QDs (Fig. 3A) depicts a homogeneous distribution of around 4 nm in diameter. Furthermore, a uniform distribution of CdS QDs on the ITO electrode was confirmed by the scanning electron micrograph (SEM) of the CdS/MB DA-PEC

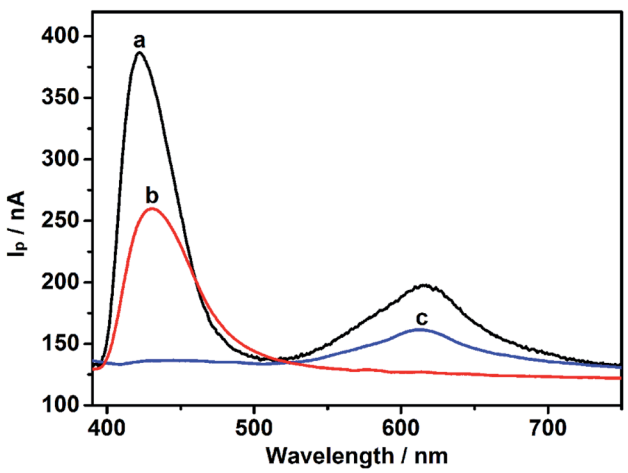

Fig. 2 I–λ curve of a wavelength-resolved CdS/MB photoelectrode (a), CdS QDs (b), and MB (c).

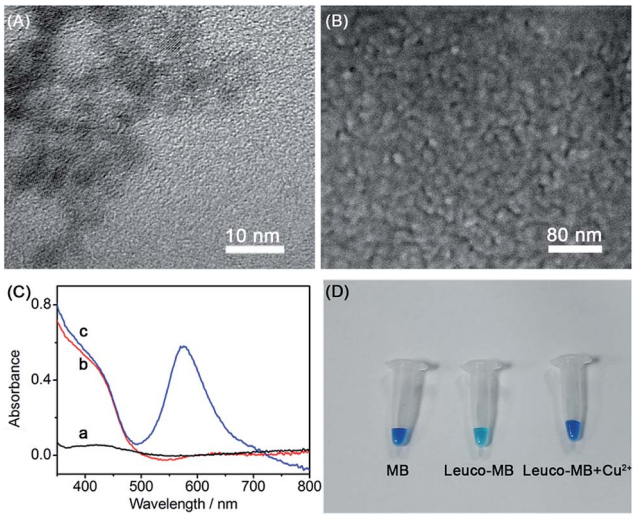

Fig. 3 (A) TEM of CdS QDs and (B) SEM image of the CdS/MB photoelectrode. (C) Absorption spectra of ITO electrode (a), CdS modified ITO electrode (b) and CdS/MB photoelectrode (c). (D) Photographs of MB, leuco-MB and oxidation products of leuco-MB catalyzed by Cu^{2+}.

photoelectrode (Fig. 3B). To study the absorption spectrum of the photoelectrode, UV-vis spectroscopic experiments on a blank ITO electrode, CdS modified ITO and a CdS/MB photoelectrode were carried out and the results obtained are shown in Fig. 3C. The spectrum of the blank ITO electrode (curve a) exhibited no obvious peaks within the experimental wavelength range, while the CdS modified ITO electrode acquired a broad absorption band below 500 nm (curve b). After absorbing MB, the CdS/MB photoelectrode showed a new absorption peak at around 600 nm (curve c). The UV-vis spectra were consistent with the I–λ curve of the CdS/MB DA-PEC photoelectrode, confirming the successful preparation of a photoelectrode. Fig. 3D depicts the color change under different conditions. In the presence of a reducing agent, MB was reduced to leuco-MB, which is less intense in color. Then the color was recovered after adding Cu^{2+}. This phenomenon can be explained as follows: Cu^{2+} first acted as a catalyst to oxidize leuco-MB to MB and was itself reduced to Cu^{+}, then the Cu^{+} was reoxidized to Cu^{2+} by dissolved oxygen in solution to give an overall catalytic oxidization of leuco-MB to MB.[34,35]

Feasibility of WR-PEC sensors

In order to evaluate the feasibility of Cu^{2+} detection, we investigated the effect of Cu^{2+} on the WR-PEC sensor. Fig. 4A shows the increase of absorption peak intensity caused by adding different concentrations of Cu^{2+} into the negatively charged leuco-MB solution due to the catalytic oxidation of leuco-MB by oxygen through the addition of a trace amount of Cu^{2+}. Hence, an increased loading of positively charged MB on the negatively charged CdS QDs *via* electrostatic interaction would increase with an increasing Cu^{2+} concentration (see ESI, Fig. S1†).

On the other hand, Fig. 4B depicts the change of the I–λ curve of a CdS modified ITO electrode incubated in 1 mM leuco-MB in the absence and presence of Cu^{2+}. The I–λ curve of the CdS

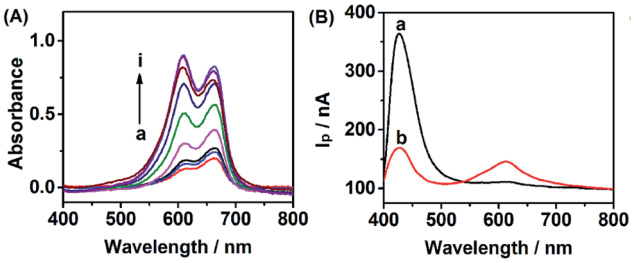

Fig. 4 (A) Absorption spectra of 1 mM leuco-MB aqueous solution incubated with different concentrations of Cu^{2+} from 0 to 0.1 mM. (B) I–λ curves of CdS modified ITO electrode incubated with 1 mM leuco-MB in the absence (a) and presence (b) of 0.1 mM Cu^{2+}.

modified ITO showed a large I_p peak of CdS and a small I_p peak of MB (curve a). After incubation with Cu^{2+}, the CdS/MB DA-PEC photoelectrode displayed an obvious decrease of the I_p of CdS and the increase of I_p of MB (curve b). This phenomenon is attributed to the fact that introducing Cu^{2+} could form exciton traps on the surface of CdS, which would quench the excitons to reduce the photocurrent of the QDs.[36] Therefore, a turn off CdS signal and a turn on MB signal could be simultaneously obtained upon the addition of Cu^{2+}. Based on the ratio of I_{pQD} and I_{pMB} (I_{pQD}/I_{pMB}), a ratiometric PEC sensor was successfully developed.

Optimization of detection conditions

Several significant parameters were determined by conducting control experiments to obtain suitable detection conditions. First, to obtain a nearly colorless leuco-MB solution, the amount of reducing agent and MB was evaluated. The molar ratios of reducing agent and MB at 10 : 1, 8 : 1, 6 : 1, 4 : 1 and 2 : 1 were tested (Fig. 5A). Obviously, at the molar ratio of 10 : 1, the color of the complex solution was lighter than that of any other ratio, which was low enough as a blank to carry out the following

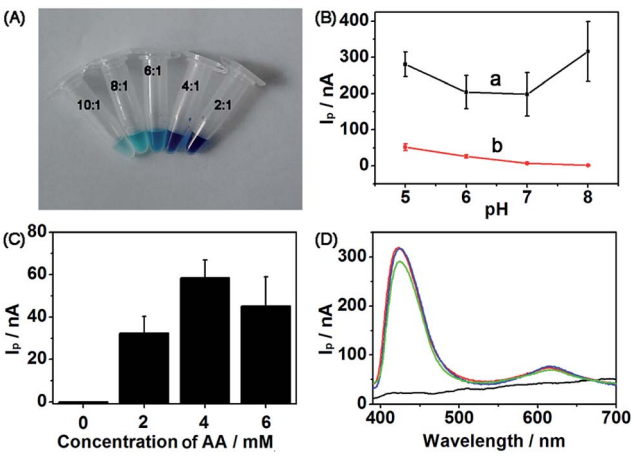

Fig. 5 (A) Photographs of 1 mM MB incubation with AA at different ratios from 10 : 1 to 2 : 1. (B) I_p of CdS (a) and MB (b) at different pHs from 5 to 8. (C) I_{pMB} at different coreactant concentrations in the detection solution. (D) I–λ curves at the different bias potentials of 0 V (black), 0.1 V (green), 0.15 V (blue) and 0.2 V (red).

experiment. I_{pQD} and I_{pMB} were measured at different pHs ranging from 5 to 8 (Fig. 5B). The I_{pMB} decreased with increasing pH. Considering that the I_p values in the CdS wavelength range were obviously stronger than those in the MB wavelength range, we chose pH 5 PBS as the detection electrolyte to improve the detection performance of the photoelectrode, in which I_{pQD}/I_{pMB} became large enough to realize ratiometric detection.

To obtain a detectable photocurrent for MB, coreactant AA was introduced to the detection electrolyte. I_{pMB} values of the CdS/MB DA-PEC photoelectrode at different concentrations of AA were measured (Fig. 5C), and naturally the concentration of 4 mM was chosen as the detection concentration according to the I_p value of MB. Finally, the I–λ curves at different bias potentials were measured to determine a suitable potential for this system (Fig. 5D). Compared with the photocurrent at 0 V (black curve), which did not show any signal, the photocurrents at 0.1 V (green curve), 0.15 V (blue curve) and 0.2 V (red curve) were large and they all showed similar amplitudes. Hence, we chose 0.1 V as the bias potential, which is close to the physiological voltage.

PEC response to Cu^{2+}

As mentioned above, the model analyte of Cu^{2+} could quench the photocurrent of QDs, and enhance the photocurrent of MB. Under optimal conditions (0.1 V bias potential, in pH 5.0 PBS with 4 mM AA), the CdS/MB DA-PEC photoelectrode was used to establish a WR-PEC sensor for Cu^{2+} based on the ratios of I_{pQD}/I_{pMB}. As shown in Fig. 6, the I_{pQD} peak at around 430 nm decreased with increasing Cu^{2+} concentration, while the I_{pMB} at 615 nm increased. A good linear relationship was established between I_{pQD}/I_{pMB} and the logarithmic value of Cu^{2+} concentration in a range from 40 nM to 0.10 mM with a correlation coefficient of 0.990 (Fig. 6, insert). The detection limit was calculated to be 0.37 nM, at a signal-to-noise ratio S/N = 3, which was lower than the analyte-induced exciton trapping method (5.9 nM),[36] and the ZnO/CdS hierarchical nanospheres based PEC (10 nM),[37] showing a good detection sensitivity.

Interference

Several common cations (Mn^{2+}, Mg^{2+}, Co^{2+}, Pb^{2+}, Ni^{2+} and Cd^{2+}) at a 10-fold concentration were chosen as interfering species to evaluate the selectivity of this wavelength-resolved ratiometric PEC sensor (Fig. 7). The photocurrent ratio in response to those cations was close to that of the blank, while the ratio for Cu^{2+} decreased to 21% of the blank. The results reveal the favorable anti-interference ability of this WR-PEC sensor.

Furthermore, the WR-PEC photoelectrode possessed a good anti-interference ability to several environmental factors such as the intensity of the light source, and the concentration of photoactive species. The photocurrents of CdS and MB obviously changed with the illumination of light on the CdS/MB DA-PEC photoelectrode. I_{pQD} under 210 Lx and 258 Lx increased 2.8 and 4.5 times compared to I_{pQD} at 138 Lx, while I_{pQD}/I_{pMB} at 210 Lx and 258 Lx only increased 1.5 and 1.7 times, respectively (see ESI, Fig. S2†). Moreover, the amount of CdS would influence the photocurrent and MB loading amount. When the volume of CdS was 8 μL and 10 μL, the I_p of CdS increased 1.3 and 1.6 times compared to 5 μL. Meanwhile, the I_{pQD}/I_{pMB} at 8 μL and 10 μL was 0.92 and 0.94 times that of 5 μL (see ESI, Fig. S3†). Therefore, compared to conventional PEC techniques, the WR-PEC exhibited better anti-interference to interfere factors, which may come from complex environmental interference or experimental operation variation.

Stability of PEC sensor

To evaluate the reliability of this system, the inter-assay precision of five as-prepared PEC sensors was examined in the presence and absence of 10 μM Cu^{2+}. The relative standard deviations (RSD) of the five measurements were 3.8% and 4.4%, respectively, demonstrating the good fabrication

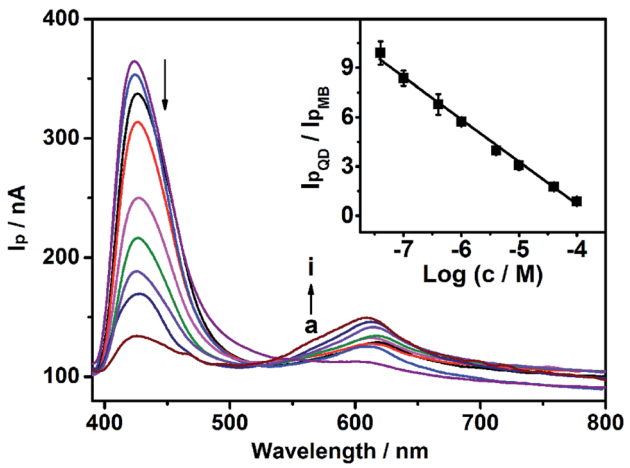

Fig. 6 I–λ curves of the optimized WR-PEC sensor in response to different concentrations of Cu^{2+}: 0, 40 nM, 100 nM, 0.4, 1.0, 4.0, 10, 40 and 100 μM (from a to i). Insert: plot of I_{pQD}/I_{pMB} *vs.* the logarithmic value of Cu^{2+} concentration.

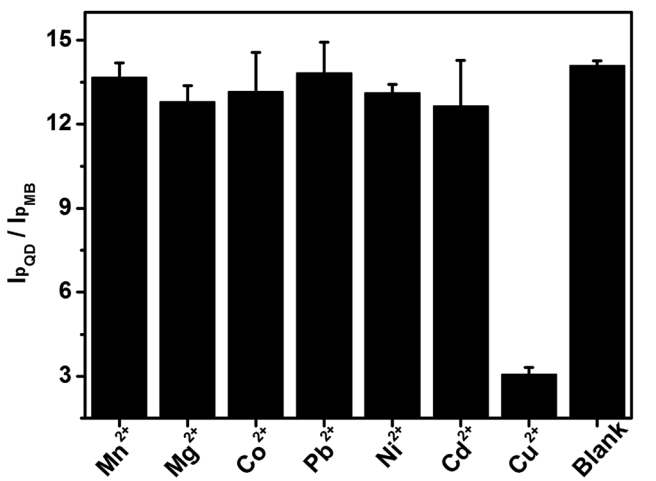

Fig. 7 I_{pQD}/I_{pMB} of the PEC sensor in response to 0.1 mM Mn^{2+}, Mg^{2+}, Co^{2+}, Pb^{2+}, Ni^{2+}, Cd^{2+}, 10 μM Cu^{2+} and buffer.

reproducibility of the PEC sensor. Meanwhile, eight scans (from 400 nm to 800 nm) for I–λ curves for one experimental process were measured for a CdS modified ITO electrode incubation with 1 mM MB (Fig. 8A), and 1 mM leuco-MB with 40 μM Cu^{2+} (Fig. 8B). The photocurrent of MB declined slightly during the experiment process, indicating acceptable stability and reliability of the PEC sensor.

Other types of WR-PEC photoelectrodes

Based on the different photocurrent directions of the photoactive species, the CdS/MgPc anodic–cathodic (AC-PEC) photoelectrode, and the CdTe/MgPc dual-cathodic (DC-PEC) photoelectrode were also established under different bias potentials. The CdS/MgPc AC-PEC photoelectrode showed three peaks at 430 nm (anodic peak, CdS QDs), 630 nm and 685 nm (cathodic peak, MgPc) under 0 V (see ESI, Fig. S4†). The CdTe/MgPc DC-PEC photoelectrode showed three peaks at 430 nm (cathodic peak, CdTe QDs), 630 nm and 685 nm (cathodic peak, MgPc) under −0.2 V (see ESI, Fig. S5†). These two types of photoelectrode also exhibited good separation of each photocurrent peak to provide potential applications in WR-PEC analysis.

Application in human hair sample

A real-life complex sample of human hair was taken to evaluate the detection effect of the WR-PEC sensor based on the CdS/MB DA-PEC photoelectrode. All human subjects were volunteers for this study, and provided informed consent. The copper element content of 12.6 ± 0.5 μg g^{-1} (n = 3) was in agreement with 12.1 ± 0.2 μg g^{-1} (n = 3) obtained using inductively coupled plasma mass spectrometry. When spiked with 2 μM, 4 μM and 8 μM Cu^{2+} standard solution, the recoveries were detected to be 102.5% ± 1.4%, 99.5% ± 3.9% and 105.1% ± 5.2%. These experimental results indicated the good reproducibility and precision of the PEC sensor.

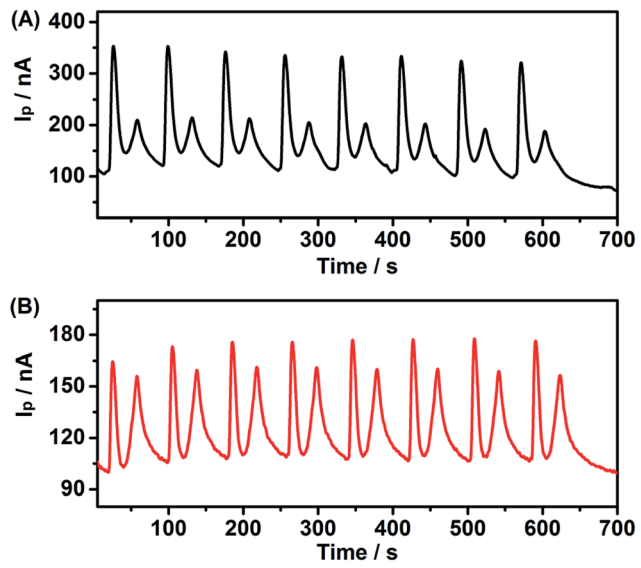

Fig. 8 Continuous PEC experiment of CdS modified ITO electrode incubation with (A) 1 mM MB and (B) 1 mM leuco-MB + 40 μM Cu^{2+}.

Conclusions

A WR-PEC technique with good sensitivity and anti-interference ability was successfully established using two PEC species with separated absorbance peaks. The WR-PEC photoelectrode was stepwise assembled with CdS QDs and MB to realize ratiometric analysis. By monitoring the ratio variation of CdS to MB, a WR-PEC sensor for a model analyte of Cu^{2+} was established. The introduction of Cu^{2+} to this sensor resulted in a "turn off" signal due to the formation of exciton trapping on the surface of CdS QDs, and a "turn on" signal of MB caused by the catalytic oxidation of Cu^{2+}. The I_{pQD}/I_{pMB} exhibited a wide linear relationship with the logarithmic value of the Cu^{2+} concentration with high sensitivity. Furthermore, the WR-PEC sensor showed excellent capacity for anti-interference, in complex environments or to experimental option variation, compared with conventional PEC approaches. More significantly, an AC-PEC photoelectrode and a DC-PEC photoelectrode with great potential in designing ratiometric sensors were also constructed to expand the application of the WR-PEC technique. The WR-PEC technique provides a new concept to design ratiometric approaches and would broaden the application of PEC sensors in biosensing and clinical diagnosis.

Experimental section

Materials and reagents

Cadmium chloride ($CdCl_2 \cdot 2.5H_2O$), ascorbic acid and magnesium phthalocyanine were purchased from Alfa Aesar China Ltd. MB and 3-mercaptopropionic acid (MPA, ≥99%) were purchased from Sigma-Aldrich (China). Cupric nitrate ($Cu(NO_3)_2 \cdot 3H_2O$) was purchased from Shanghai Sinpeuo Fine Chemical Co., Ltd. (China). All other chemicals were of analytical grade without further purification. In our work, 0.1 M phosphate buffer salines (PBS) at different pH were prepared by mixing 0.1 M NaH_2PO_4 and 0.1 M Na_2HPO_4 stocks containing 0.1 M NaCl as the supporting electrolyte. An HAc–NaAc (0.01 M, pH 4.0) buffer was used to prepare Cu^{2+} solution. ITO coated glasses were used as an electrode material and were purchased from Zhuhai Kaivo Electronic Components Co., Ltd, they were cut into 4.4 cm × 1.2 cm slices. Ultrapure water (≥18 MΩ, Milli-Q, Millipore) was used throughout the experiment.

The human hair sample was digested using a mixture of 70% (W/W) nitric acid and 60% (W/W) perchloric acid (3 : 1 V/V). The resulting sample solution was diluted and neutralized to pH 4 using 0.5 M NaOH prior to detection.

Apparatus

The SEMs were acquired using a Hitachi S-4800 scanning electron microscope (Japan) while TEMs were recorded using a JEM-2100 TEM instrument (JEOL, Japan). The UV-vis absorption spectra were obtained using a UV-3600 UV-vis-NIR spectrophotometer (Shimadzu Co., Kyoto, Japan). Photoelectrochemical

measurements were performed with a home-built photoelectrochemical system. A 500 W Xe lamp equipped with a monochromator was used as the irradiation source. The photocurrent was measured on a CHI 630D electrochemical workstation (CH Instruments, Austin, TX). A grating spectrometer Omni-λ1509 (Beijing Zolix Instruments CO., LTD) was used to obtain a continuous wavelength spectrum. All modified processes were performed at 37 °C, and all PEC experiments were carried out at room temperature using a conventional three-electrode system, with a modified ITO electrode as the working electrode, a platinum wire as the counter electrode and a saturated Ag/AgCl electrode as the reference electrode.

Preparation of MPA–CdS QDs

Water-soluble MPA stabilized CdS QDs were prepared according to a previously described method.[38] Briefly, 90 μL of MPA was added to 20 mL of 20 mM $CdCl_2$ solution. Next, 1 M sodium hydroxide solution was used to adjust the pH of the solution to 10. Under extensive stirring in air at room temperature, 20 mL of 20 mM thioacetamide solution was added slowly and stirred continuously for 30 min. Then the resultant solution was refluxed at 80 °C for 10 h to obtain CdS QD solution. After purification and drying, the precipitate was redispersed with ultrapure water. Finally, the product was kept at 4 °C before use.

Fabrication of WR-PEC sensors

For preparation of the CdS/MB DA-PEC photoelectrode, ITO slices were first cleaned by immersion in 0.5 M NaOH for 10 min and 10% H_2O_2 for another 10 min. After immersion in acetone for 30 min, ITO slices were washed by ultrapure water, and dried. 5 μL of the as-prepared CdS QD solution was dropped onto the ITO electrode and dried at 37 °C to obtain a CdS modified photoelectrode. After the washing and drying process, 10 μL of 1 mM MB solution was dropped onto the CdS modified photoelectrode, and bathed in a high humidity environment at room temperature for 1 h, followed by washing with water. Finally, the photoelectrode was dried at 37 °C to obtain the CdS/MB DA-PEC photocathode through electrostatic interaction. For a CdS/MgPc AC-PEC photoelectrode or CdTe/MgPc DC-PEC photoelectrode, 10 μL of 2 mg mL^{-1} MgPc in DMF was mixed with 10 μL of 0.25 mg mL^{-1} chitosan solution, and dropped on the ITO slice and then coated with 20 μL of as-prepared CdS or CdTe solution, respectively.

PEC detection of Cu^{2+}

Leuco-MB solution was prepared by adding 10 μL of 10 mM reducing agent (AA) to 10 μL of 1 mM MB solution, and kept at room temperature for 10 min. For Cu^{2+} detection, 5 μL of CdS QDs was applied to an ITO slice, and dried at 37 °C, followed by washing with water. Then, 10 μL of 1 mM leuco-MB solution was mixed with 10 μL of a Cu^{2+} standard stock solution, and 20 μL of the mixture solution was applied to the CdS modified photoelectrode. This was then left for 1 h at room temperature. After rinsing three times with deionized water, the as-prepared sensor was used for PEC detection in air-saturated PBS (0.1 M, pH 5.0) containing 4 mM AA as coreactant at a 0.1 V bias potential.

Acknowledgements

We gratefully acknowledge the National Natural Science Foundation of China (21375060, 21135002, 21121091) and Priority development areas of National Research Foundation for the Doctoral Program of Higher Education of China (20130091130005).

Notes and references

1 L. M. Zhang, Y. Y. Han, F. Zhao, G. Y. Shi and Y. Tian, *Anal. Chem.*, 2015, **87**, 2931–2936.
2 K. W. Ren, J. Wu, F. Yan and H. X. Ju, *Sci. Rep.*, 2014, **4**, 4360–4366.
3 X. L. Chai, L. M. Zhang and Y. Tian, *Anal. Chem.*, 2014, **86**, 10668–10673.
4 L. Yuan, F. P. Jin, Z. B. Zeng, C. B. Liu, S. L. Luo and J. S. Wu, *Chem. Sci.*, 2015, **6**, 2360–2365.
5 S. Sreejith, K. P. Divya and A. Ajayaghosh, *Angew. Chem., Int. Ed.*, 2008, **47**, 7883–7887.
6 X. L. Zhang, Y. Xiao and X. H. Qian, *Angew. Chem., Int. Ed.*, 2008, **47**, 8025–8029.
7 C. S. Huang, T. Jia, M. F. Tang, Q. Yin, W. P. Zhu, C. Zhang, Y. Yang, N. Q. Jia, Y. F. Xu and X. H. Qian, *J. Am. Chem. Soc.*, 2014, **136**, 14237–14244.
8 X. Wang, J. Sun, W. H. Zhang, X. X. Ma, J. Z. Lv and B. Tang, *Chem. Sci.*, 2013, **4**, 2551–2556.
9 Y. Cheng, Y. Huang, J. P. Lei, L. Zhang and H. X. Ju, *Anal. Chem.*, 2014, **86**, 5158–5163.
10 H. R. Zhang, J. J. Xu and H. Y. Chen, *Anal. Chem.*, 2013, **85**, 5321–5325.
11 S. G. Sun, W. Sun, D. Z. Mu, N. Jiang and X. J. Peng, *Chem. Commun.*, 2015, **51**, 2529–2531.
12 W. W. Zhao, J. J. Xu and H. Y. Chen, *Chem. Rev.*, 2014, **114**, 7421–7441.
13 W. W. Zhan, Q. Kuang, J. Z. Zhou, X. J. Kong, Z. X. Xie and L. S. Zheng, *J. Am. Chem. Soc.*, 2013, **135**, 1926–1933.
14 N. Haddour, J. Chauvin, C. Gondran and S. Cosnier, *J. Am. Chem. Soc.*, 2006, **128**, 9693–9698.
15 W. G. Ma, D. X. Han, M. Zhou, H. Sun, L. N. Wang, X. D. Dong and L. Niu, *Chem. Sci.*, 2014, **5**, 3946–3951.
16 J. Tang, B. Kong, Y. C. Wang, M. Xu, Y. L. Wang, H. Wu and G. F. Zheng, *Nano Lett.*, 2013, **13**, 5350–5354.
17 W. W. Zhao, Z. Y. Ma, P. P. Yu, X. Y. Dong, J. J. Xu and H. Y. Chen, *Anal. Chem.*, 2012, **84**, 917–923.
18 D. Chen, H. Zhang, X. Li and J. H. Li, *Anal. Chem.*, 2010, **82**, 2253–2261.
19 J. M. Gong, X. Q. Wang, X. Li and K. W. Wang, *Biosens. Bioelectron.*, 2012, **26**, 43–49.
20 X. Q. Liu, A. Niazov-Elkan, F. Wang and I. Willner, *Nano Lett.*, 2013, **13**, 219–225.
21 X. X. Zeng, S. S. Ma, J. C. Bao, W. W. Tu and Z. H. Dai, *Anal. Chem.*, 2013, **85**, 11720–11724.

22 F. X. Xiao, J. Miao and B. Liu, *J. Am. Chem. Soc.*, 2014, **136**, 1559–1569.
23 X. R. Zhang, S. G. Li, X. Jin and S. S. Zhang, *Chem. Commun.*, 2011, **47**, 4929–4931.
24 D. Dong, D. Zheng, F. Q. Wang, X. Q. Yang, N. Wang, Y. G. Li, L. H. Guo and J. Cheng, *Anal. Chem.*, 2003, **76**, 499–501.
25 W. W. Tu, Y. T. Dong, J. P. Lei and H. X. Ju, *Anal. Chem.*, 2010, **82**, 8711–8716.
26 M. Kato, T. Cardona, A. W. Rutherford and E. Reisner, *J. Am. Chem. Soc.*, 2012, **134**, 8332–8335.
27 N. Karousis, J. Ortiz, K. Ohkubo, T. Hasobe, S. Fukuzumi, Á. Sastre-Santos and N. Tagmatarchis, *J. Phys. Chem. C*, 2012, **116**, 20564–20573.
28 J. Bartelmess, B. Ballesteros, G. de la Torre, D. Kiessling, S. Campidelli, M. Prato, T. Torres and D. M. Guldi, *J. Am. Chem. Soc.*, 2010, **132**, 16202–16211.
29 J. A. Cooper, M. Wu and R. G. Compton, *Anal. Chem.*, 1998, **70**, 2922–2927.
30 A. J. Nozik, M. C. Beard, J. M. Luther, M. Law, R. J. Ellingson and J. C. Johnson, *Chem. Rev.*, 2010, **110**, 6873–6890.
31 X. Y. Yu, B. X. Lei, D. B. Kuang and C. Y. Su, *Chem. Sci.*, 2011, **2**, 1396–1400.
32 R. Gill, M. Zayats and I. Willner, *Angew. Chem., Int. Ed.*, 2008, **47**, 7602–7625.
33 J. A. Cooper, K. E. Woodhouse, A. M. Chippindale and R. G. Compton, *Electroanalysis*, 1999, **11**, 1259–1265.
34 M. N. Khan and A. Sarwar, *Anal. Sci.*, 2001, **17**, 1195–1197.
35 O. Impert, A. Katafias, P. Kita, A. Mills, A. Pietkiewicz-Graczyk and G. Wrzeszcz, *Dalton Trans.*, 2003, **3**, 348–353.
36 P. Wang, X. Y. Ma, M. Q. Su, Q. Hao, J. P. Lei and H. X. Ju, *Chem. Commun.*, 2012, **48**, 10216–10218.
37 Q. M. Shen, X. M. Zhao, S. W. Zhou, W. H. Hou and J. J. Zhu, *J. Phys. Chem. C*, 2011, **115**, 17958–17964.
38 E. Han, L. Ding, S. Jin and H. X. Ju, *Biosens. Bioelectron.*, 2011, **26**, 2500–2505.